



## Comparison of two types of persistent heavy rainfall events during sixteen warm seasons in the Sichuan Basin

Yuanchun Zhang <sup>a,\*</sup>, Jianhua Sun <sup>a</sup>, Luqi Zhu <sup>b</sup>, Huan Tang <sup>b</sup>, Shuanglong Jin <sup>c,d</sup>, Xiaolin Liu <sup>c,d</sup>

<sup>a</sup> Key Laboratory of Cloud-Precipitation Physics and Severe Storms (LACS), Institute of Atmospheric Physics, Chinese Academy of Sciences, Beijing, China

<sup>b</sup> College of Atmospheric Sciences, Lanzhou University, Lanzhou, China

<sup>c</sup> State Key Laboratory of Operation and Control of Renewable Energy & Storage Systems, China Electric Power Research Institute, Beijing, China

<sup>d</sup> Electric Power Meteorology State Grid Corporation Joint Laboratory (CEPRI), Beijing, China

### ARTICLE INFO

#### Keywords:

Southwest vortex  
Persistent heavy rainfall event  
Large-scale circulation  
Vorticity budget  
关键词:  
西南低涡  
持续性暴雨  
大尺度环流  
涡度收支

### ABSTRACT

Based on hourly precipitation from national surface stations, persistent heavy rainfall events (PHREs) over the Sichuan Basin (SCB) are explored during the warm season (May to September) from 2000 to 2015 to compare synoptic circulations and maintenance mechanisms between different PHRE types. There are two main types of PHREs: one is characterized by a rain belt west of 106°E over the SCB (WSB-PHREs), and the other features a rain belt east of 106°E over the SCB (ESB-PHREs). In total, there are 18 ESB-PHREs and 10 WSB-PHREs during the study period. Overall, the rain belts of WSB-PHREs are along the terrain distribution east of the Tibetan Plateau, while the precipitation intensity of ESB-PHREs is stronger. For the two types of PHREs, the shortwave trough over the SCB and the western Pacific subtropical high act as their favorable background environments, particularly for ESB-PHREs. The water vapor of WSB-PHREs is mainly transported from the South China Sea, whereas for ESB-PHREs the South China Sea and Bay of Bengal are their main moisture sources. The composite vorticity budgets of southwest vortices during their mature stage indicate that the convergence effect is a dominant factor for maintaining the two types of PHREs, and the strong vertical vorticity advection is also favorable, but the relative contribution of vertical advection is larger for WSB-PHREs.

#### 摘要

本文筛选出四川盆地西部(盆西型)和盆地东部(盆东型)持续性暴雨个例,深入对比两类持续性暴雨的大气环流特征和直接造成持续性暴雨的西南低涡维持的机理。四川盆地的短波槽和西太平洋副热带高压的配置有利于持续性暴雨的维持,盆东型的降水强度较盆西型个例强,高空急流位置偏南,南亚高压的强度更强,高层辐散更强,对流层中层副热带高压偏东偏南。盆西型的水汽输送主要来自南海,而盆东型的水汽输送主要来自南海和孟加拉湾。合成涡度收支的结果表明散度项是两类持续暴雨中西南涡维持的主要原因,但盆西型中,垂直平流的作用更强。

### 1. Introduction

Persistent heavy rainfall events (PHREs) can cause particularly severe disasters in China, such as flash floods, urban waterlogging, or landslides (Kunkel et al., 1994; Grazzini and Grijin, 2003; Zhao et al., 2004; Schumacher, 2011; Jiang et al., 2017). In China, many different definitions of a PHRE have been developed based on various rainfall datasets (Tao, 1980; Bao, 2007; Wang et al., 2014; Liu et al., 2019). The Sichuan Basin (SCB) is in a subtropical region east of the eastern edge of the Tibetan Plateau (TP) and west of the Wushan and Daba mountains. Because of the complexity of its topography and climatic background, the SCB is one of the frequent heavy rainfall regions in China. PHREs in the SCB have been defined as having a rainfall duration of more than 48 h and a continuous daily precipitation of more than 50

mm (Chen et al., 2010); however, research has mostly been in the form of case studies. Statistical results are still lacking in terms of explaining the features of PHREs in recent decades. Previous studies found that the apparent spatial distribution of rainfall anomalies in the SCB has an east-west oscillation (Shao et al., 2005; Bai et al., 2011; Liao et al., 2012; Li et al., 2016; Jiang et al., 2017). For the rainfall in the western SCB (WSB), the circulation at mid-to-high latitudes has two ridges and one trough. The southwest vortices are active and the western Pacific subtropical high (WPSH) is located west and north of its average location (Zhou et al., 2008). For the rainfall in the eastern SCB (ESB), the meridional background circulation controls the mid-to-high latitudinal regions. A low trough appears over the SCB and the vortices in the middle of the basin move eastward (Zhou et al., 2008; Bai et al., 2011). Other studies have found that water vapor transport is also im-

\* Corresponding author.

E-mail address: [zhyc@mail.iap.ac.cn](mailto:zhyc@mail.iap.ac.cn) (Y. Zhang).

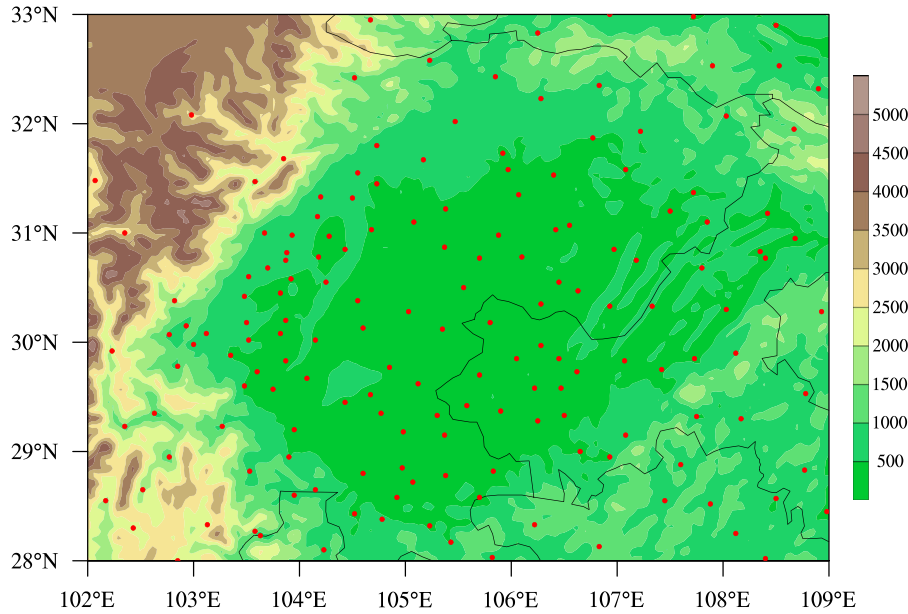


**Fig. 1.** Geographic distribution of the 163 surface stations (red dots). Colored shading indicates the terrain height (units: m).

portant in determining the rain belt location (Li et al., 2016; Jiang et al., 2017).

Some case studies have focused on PHREs in the SCB and the mechanisms that control these events, but few studies have considered the statistical features of PHREs in the SCB. This study focuses on warm-season PHREs in the SCB in recent decades and a comparison of the maintenance mechanisms of the two types of PHREs, with a particular focus on exploring the vorticity evolution mechanism of SWVs that directly trigger PHREs. **Section 2** introduces the data and methods. **Section 3** presents the definitions and categories of PHREs in the SCB. **Section 4** compares the maintenance mechanisms of the two types of PHREs. **Section 5** concludes the paper.

## 2. Data and methods

Hourly precipitation observations from surface stations operated by the China Meteorological Administration are used to examine PHREs in the SCB during the warm season (May to September) from 2000 to 2015 (**Fig. 1**). The study area covers the region of 28°–33°N and 102°–109°E. Because data are missing at some stations, two strict quality control conditions are adopted: (1) the missing hourly precipitation data have to be less than 2% of the total data series in each year and there should be no missing year of hourly precipitation at each station; (2) the stations located at a terrain height greater than 2500 m are not used to avoid interference from stations on the TP. After this quality control procedure, 163 stations are left in the study area (red dots in **Fig. 1**). The hourly ERA5 reanalysis data with a horizontal resolution of 0.25° are used to compare the large-scale circulation and calculate the SWV vorticity budget of the two types of PHREs.

The vorticity budget equation below is used to explore the maintenance mechanism of SWVs during their mature stage:

$$\frac{\delta \zeta_z}{\delta t} = -\mathbf{V}_h \cdot \nabla_h \zeta_z - w \frac{\partial \zeta_z}{\partial z} + \mathbf{k} \cdot \left( \frac{\partial \mathbf{V}_h}{\partial z} \times \nabla_h w \right) - (\zeta_z + f) \nabla_h \cdot \mathbf{V}_h + \text{RES},$$

LHS	HADV	VADV	TILT	DIV	(1)
-----	------	------	------	-----	-----

where  $\zeta_z$  is the vertical vorticity and  $\delta$  is the vorticity tendency.  $w$  is the vertical velocity and  $t$  is the time. The term  $\mathbf{V}_h = u\mathbf{i} + v\mathbf{j}$  is the horizontal velocity vector, where  $\mathbf{i}$ ,  $\mathbf{j}$ , and  $\mathbf{k}$  stand for the unit vector components pointing to the east, north, and zenith;  $\nabla_h = \frac{\partial}{\partial x}\mathbf{i} + \frac{\partial}{\partial y}\mathbf{j}$  is the horizontal gradient operator; and  $f$  is the Coriolis parameter. The term HADV represents the horizontal advection of vorticity, VADV denotes the vertical

**Table 1** Definition of PHREs in the SCB.

Features	Definition
Intensity	Concentrated torrential rainfall stations identified each day.
Coverage	More than 10 concentrated torrential rainfall stations identified on at least one day and more than 8 concentrated torrential rainfall stations identified over the other two days.
Duration	More than three days.
Overlap	The overlap of the heavy rainfall stations should be more than 30% on two consecutive days.

advection of vorticity, TILT is the tilting term, DIV is the stretching effect associated with divergence or convergence, and RES is the residual term. The term on the left-hand side (LHS) is the vorticity tendency, and the sum of the terms other than RES on the right-hand side is denoted as RHS.

## 3. PHREs in the SCB

### 3.1. Definition of PHREs

Because PHREs are always regional rainfall events, their definition is affected by the selection of surface stations. A torrential rainfall station is a single station with a daily precipitation  $\geq 50$  mm and a heavy rainfall station has a daily precipitation  $\geq 25$  mm. To remove the influence of scattered and isolated stations, a definition of concentrated stations has been proposed (Wang et al., 2016): when more than three torrential (heavy) rainfall stations occur within a distance of less than 100 km to a torrential (heavy) rainfall station, this torrential (heavy) rainfall station is defined as a concentrated torrential (heavy) rainfall station. Regionally, PHREs in the SCB are defined as follows (**Table 1**): (1) heavy rainfall events lasting for more than three days; (2) more than 10 concentrated torrential rainfall stations identified on at least one day and more than 8 concentrated torrential rainfall stations identified over the other two days; (3) regionally heavy rainfall is spatially continuous, and the overlap of the heavy rainfall stations should therefore be greater than 30% for two consecutive days.

### 3.2. Categories of PHREs

Based on the definition of PHREs given above, 33 cases are selected during the warm season from 2000 to 2015. According to the results of

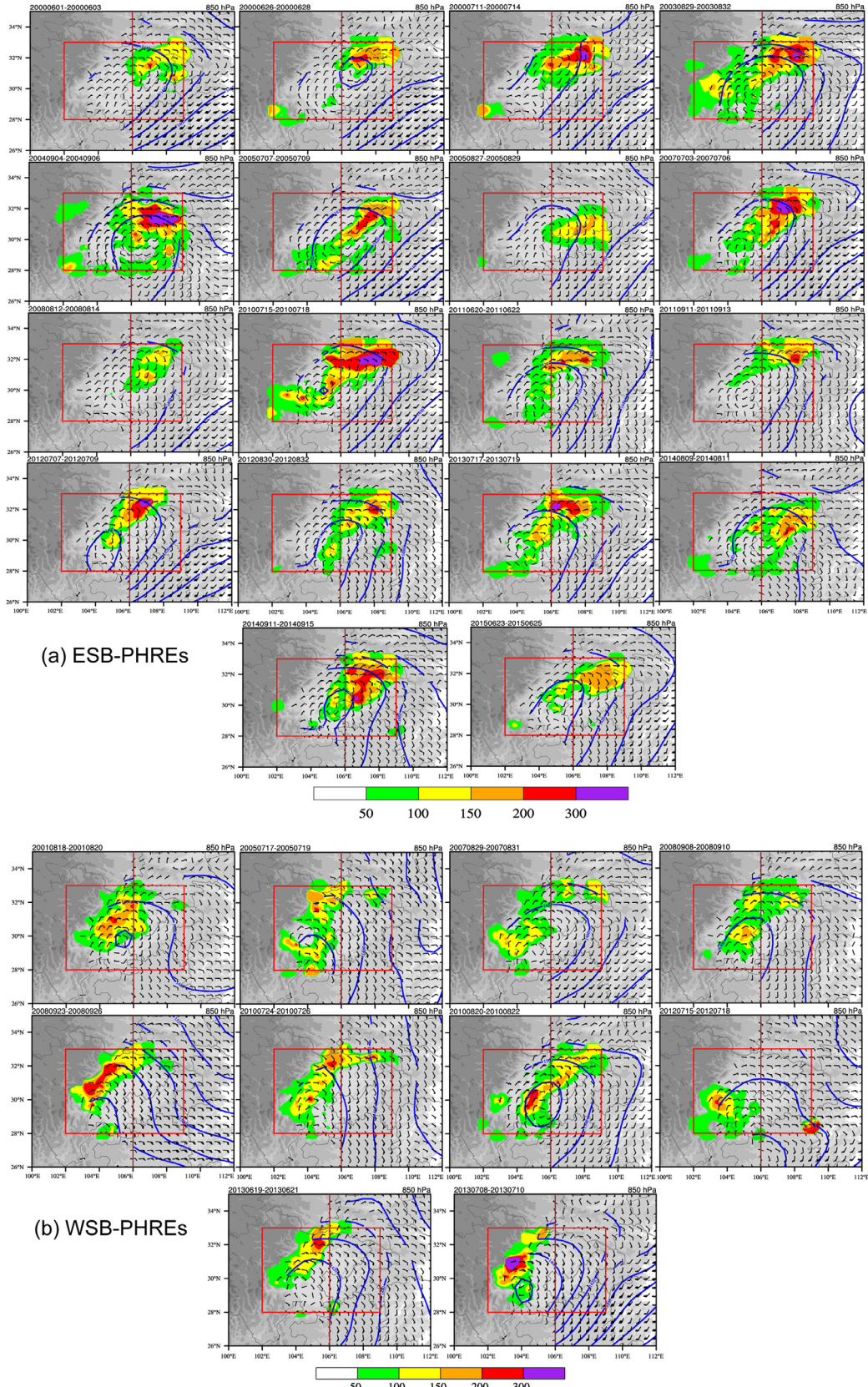


**Fig. 2.** Total precipitation (shading; units: mm), average wind field (black wind barbs), and geopotential height (blue solid lines; units: gpm) at 850 hPa of each PHRE: (a) ESB-PHREs; (b) WSB-PHREs. The red frame is where the vorticity budget is calculated and the deep red line is the location of 106°E. Gray shading indicates the terrain height (units: m).

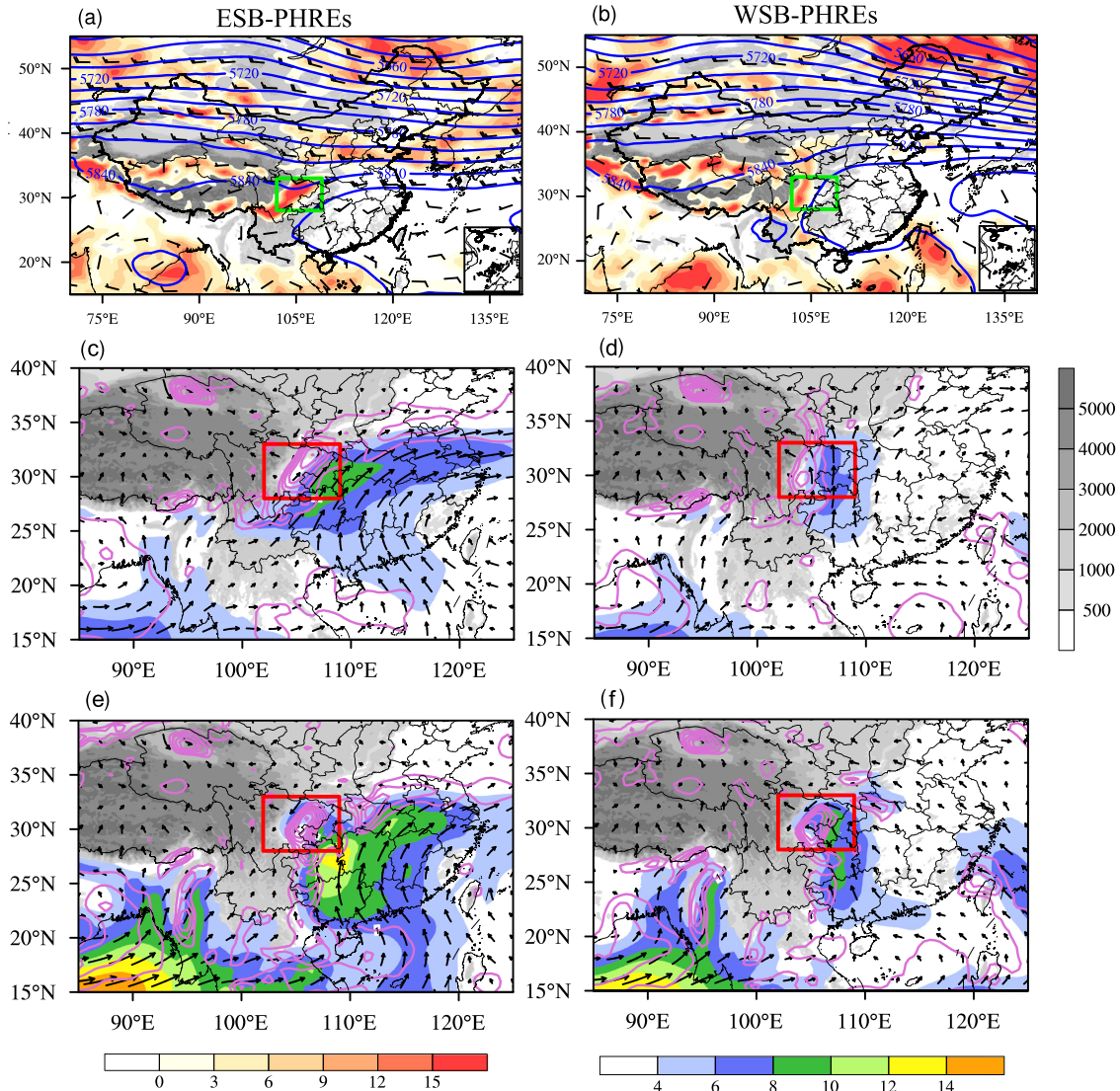


**Fig. 3.** Composite circulation at (a, b) 500 hPa, (c, d) 700 hPa, and (e, f) 850 hPa: (a, c, e) ESB-PHREs; (b, d, f) WSB-PHREs. In (a, b), the green frame is the study area, color shading shows the vorticity (units:  $10^{-6} \text{ s}^{-1}$ ), blue lines show the geopotential height (units: gpm), and the vectors show the wind field. In (c–f), color shading shows the water vapor flux (units:  $\text{g s kg}^{-1}$ ), purple lines show the vorticity (units:  $10^{-5} \text{ s}^{-1}$ ), vectors show the wind field, and the red frame is the study area. Gray shading denotes the terrain height (units: m).

**Table 2** The dates of ESB- and WSB-PHREs during the warm season of 2000–2015.

Types	Dates
ESB-PHREs	1–3 Jun 2000; 26–28 Jun 2000; 11–14 Jul 2000; 29 Aug–1 Sep 2003; 4–6 Sep 2004; 7–9 Jul 2005; 27–29 Aug 2005; 3–6 Jul 2007; 12–14 Aug 2008; 15–18 Jul 2010; 20–22 Jun 2011; 11–13 Sep 2011; 7–9 Jul 2012; 30 Aug–1 Sep 2012; 17–19 Jul 2013; 9–11 Aug 2014; 11–15 Sep 2014; 23–25 Jul 2015
WSB-PHREs	1–2 Aug 2001; 17–19 Jul 2005; 29–31 Aug 2007; 8–10 Sep 2008; 23–26 Sep 2008; 24–26 Jul 2010; 20–22 Aug 2010; 15–18 Jul 2012; 19–21 Jun 2013; 8–10 Jul 2013

previous studies (Yu, 1984) and the rain belts of the selected PHREs in section 4.1, when the center of the precipitation maximum of the PHREs is located west (east) of 106°E, the events are classified as the WSB (ESB) type. As a result, 28 of the 33 PHREs are identified as either WSB- or ESB-PHREs, with 18 being ESB and 10 being WSB (Table 2). The number of ESB-PHREs is nearly twice as many as that of WSB events. From the total precipitation of each PHRE (Fig. 2), the orientation of ESB-PHREs

is found to always be northeast–southwest and their total precipitation is greater than that of WSB-PHREs. The WSB rain belts occur in regions with a large terrain height gradient along the topographic distribution.

#### 4. Comparison of maintenance mechanisms of the two types of PHREs

##### 4.1. Composite background circulation

Synoptic systems provide favorable dynamic and thermal background circulations for heavy rainfall, and mesoscale systems can directly trigger the occurrence of heavy rainfall (Ding, 1991). The composite circulations of the two types of PHREs at 500 hPa (Fig. 3(a, b)) have different features in the low-to-mid latitudes. For ESB-PHREs, the westerly wind controls the mid-to-high latitudinal regions (Fig. 3(a)). The southwesterly wind in front of the low trough (east of the TP) and peripheral regions of the WPSH cover the eastern part of the SCB, which is consistent with the strong convergence and positive vorticity maxima (Fig. 3(a)). The WPSH of WSB-PHREs extends westward to about 102°E. The western part of the SCB is controlled by the southwest-

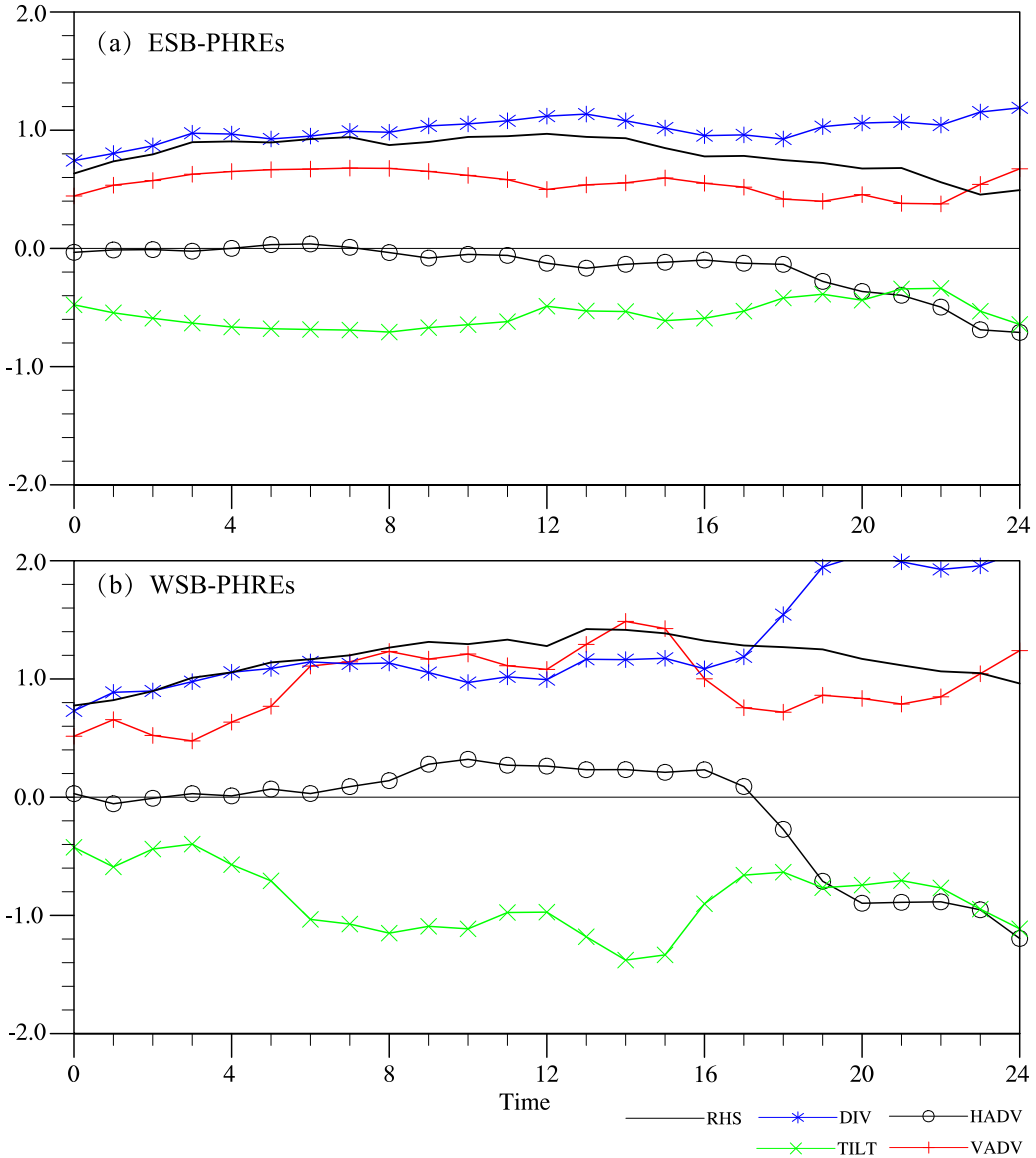


**Fig. 4.** Composite vorticity budgets of Eq. (1) averaged over the box in Fig. 3: (a) ESB-PHREs; (b) WSB-PHREs. RHS is the sum of the terms on the right-hand side; TILT stands for the tilting; DIV is short for the stretching effect of divergence or convergence; VADV is the vertical advection of vorticity; HADV is the horizontal advection of vorticity (units:  $10^{-9} \text{ s}^{-2}$ ).

early wind of the WPSH (Fig. 3(b)). It is found that the locations of the WPSH determines the rain-belt locations. When the WPSH extends westward to the ESB, the rain belt is maintained over the WSB, and while the WPSH retreats eastward and southward, combining with the low trough over the SCB, convection and the rain belt tend to occur in the ESB.

Besides the background circulations at middle levels of the troposphere, water vapor transportation at the lower levels (850 and 700 hPa) is also important for the maintenance of PHREs. For ESB-PHREs, the ESB is controlled by a southwesterly wind at 700 hPa (Fig. 3(c)). The strong water vapor flux at 850 hPa from both the Bay of Bengal and South China Sea is imported into the ESB (Fig. 3(e)). The maximum wind field of WSB-PHREs appears from the SCB to the second-step terrain, which is weaker than that of ESB-PHREs. The southerly wind on the periphery of the WPSH transports water vapor from the South China Sea into the SCB (Fig. 3(d, f)). It is indicated that the convergence and positive vorticity maximum of WSB-PHREs occur in the western part of the SCB, and the southeastern and southern winds import water vapor from the South China Sea into western regions of the SCB; however, the con-

vergence and vorticity maximum of ESB-PHREs is stronger. There are two water vapor transportation trajectories providing abundant water vapor for the ESB-PHREs: one mainly originates from the Bay of Bengal and is imported by the southwestern wind; the other is from the South China Sea and is transported by the southeastern and southern wind.

#### 4.2. Composite vorticity budgets of SWVs

As described above, the synoptic systems provide favorable dynamic and thermal background circulations for the maintenance of PHREs, but the SWV (mesoscale systems) can directly trigger the occurrence of PHREs (Fu et al., 2015, 2019; Tang et al., 2020). The average wind field at 850 hPa during each PHRE in Fig. 3 shows that most of the PHREs are related with SWVs, especially for the stronger PHREs. For ESB-PHREs (Fig. 2(a)), the SWVs tend to locate east of 106°E. However, the SWV's centers of WSB-PHREs concentrate on the eastern edge of TP. Since the PHREs are always related to the mature SWV, the 24-h mature stage of each SWV during these PHREs are chosen for the following composite analysis. To compare the dynamics that govern the intensifi-

cation and maintenance of SWVs between the two types of PHREs, the SWV vorticity budgets of each PHRE are calculated ((Eq. (1)) and the composite vorticity budgets (Fu et al., 2016) of the two types of PHREs are illustrated in Fig. 4. For both PHRE types, the vorticity of the SWV is increasing in the mature stage. DIV and VADV are positive to the intensification of SWVs, but TILT is the negative effect. The HADV is much weaker in the first 17 h. However, the VADV positive effect of WSB-PHREs is much stronger than that of ESB-PHREs from the sixth to sixteenth hour of the mature stage. This means that the vertical advection is stronger due to the intense vertical motion near the leeside of the TP with the considerable terrain gradient. However, for the maintenance of the SWV in ESB-PHREs, the convergence of southerly wind is more important in the ESB.

## 5. Conclusions

Hourly precipitation from 163 surface stations is used to investigate PHREs in the SCB during the warm season from 2000 to 2015. According to the rain belt locations, most PHREs can be categorized as either ESB or WSB types. Detailed comparisons are made for these two types of PHREs, and the main findings are as follows:

Based on the PHRE definition, 10 PHREs occur over the WSB, while 18 PHREs occur over the ESB. The WSB-PHREs rain belts distribute along with the direction of the topographic height, and the total precipitation of ESB-PHREs is greater than that of WSB-PHREs. When the WPSH extends westward to the ESB, the PHREs occur over the WSB; whereas, when the WPSH covers the second-step terrain and combines with a low trough over the SCB, the PHREs occur over the ESB. The water vapor of ESB-PHREs originates from the South China Sea and the Bay of Bengal, while the water vapor of WSB-PHREs is mainly from the South China Sea. The stronger precipitation of ESB-PHREs is related to the stronger convergence and water vapor flux.

SWVs are the main mesoscale systems for triggering PHREs. The production of cyclonic vorticity due to convergence dominates the mature stage of SWVs for both types. Additionally, strong vertical vorticity advection due to convection also plays an important role in the maintenance of SWVs, but the relative contribution of vertical advection is larger for WSB-PHREs.

This study investigates WSB- and ESB- PHREs in the SCB, and compares their background circulation, water vapor features, and SWVs' maintenance mechanisms between the two types. We believe that, in addition to SWVs, there are also other systems that directly induce PHREs in the SCB. These will be investigated in the future to reach a more comprehensive understanding of PHREs in the SCB.

## Disclosure statement

No potential conflict of interest was reported by the authors.

## Funding

This work was supported by the National Key R&D Program of China [grant number 2018YFC0809400] and the National Natural Science Foundation of China [grant number 41975057].

## References

- Bai, Y.Y., Zhang, Y., Gao, Y.H., He, Z.N., Li, Y.H., 2011. Spatial differences of precipitation over Sichuan Basin. *Scient. Geograph. Sin.* 31, 479–483. doi:[10.13249/j.cnki.sgs.2011.04.018](https://doi.org/10.13249/j.cnki.sgs.2011.04.018), (in Chinese).
- Bao, M., 2007. The statistical analysis of the persistent heavy rain in the last 50 years over China and their backgrounds on the large scale circulation. *Chinese J. Atmos. Sci.* 31, 780–781. doi:[10.3878/j.issn.1006-9895.2007.05.03](https://doi.org/10.3878/j.issn.1006-9895.2007.05.03), (in Chinese).
- Chen, Y.R., Shi, R., Li, Y.Q., Wang, C.G., 2010. The study of a kind of circulation characters on sustaining heavy rain in Sichuan Basin. *Plateau Mount. Meteorol. Res.* 30, 30–34. doi:[10.3969/j.issn.1674-2184.2010.01.005](https://doi.org/10.3969/j.issn.1674-2184.2010.01.005), (in Chinese).
- Ding, Y.H., 1991. Advanced meteorology. *China Meteorological Press, Beijing*, pp. 1–585 (in Chinese).
- Fu, S.M., Li, W.L., Sun, J.H., Zhang, J.P., Zhang, Y.C., 2015. Universal evolution mechanisms and energy conversion characteristics of long-lived mesoscale vortices over the Sichuan Basin. *Atmos. Sci. Lett.* 16, 127–134. doi:[10.1002/asl2.533](https://doi.org/10.1002/asl2.533).
- Fu, S.M., Zhang, J.P., Sun, J.H., Zhao, T.B., 2016. Composite analysis of long-lived mesoscale vortices over the middle reaches of the Yangtze River valley: Octant features and evolution mechanisms. *J. Clim.* 29, 761–781. doi:[10.1175/JCLI-D-15-0175.1](https://doi.org/10.1175/JCLI-D-15-0175.1).
- Fu, S.M., Mai, Z., Sun, J.H., Li, W.L., Ding, Y., Wang, Y.Q., 2019. Impacts of convective activity over the Tibetan Plateau on plateau vortex, southwest vortex, and downstream precipitation. *J. Atmos. Sci.* 76, 3803–3830. doi:[10.1175/JAS-D-18-0311](https://doi.org/10.1175/JAS-D-18-0311).
- Grazzini, F., Grijin, G.V.D., 2003. Central European floods during summer 2002. *ECMWF Newsletter* 96, 18–28. <https://www.ecmwf.int/node/14628>.
- Jiang, X.W., Li, Y.Q., Li, C., Du, J., 2017. Characteristics of summer water vapor transportation in Sichuan Basin and its relationship with regional drought and flood. *Plateau Meteorol.* 37, 17–18. doi:[10.3321/j.issn:1000-0534.2007.03.006](https://doi.org/10.3321/j.issn:1000-0534.2007.03.006), (in Chinese).
- Kunkel, K.E., Changnon, S.A., Angel, J.R., 1994. Climatic aspects of the 1993 Upper Mississippi River Basin flood. *Bull. Am. Meteorol. Soc.* 75 (5), 811–822. doi:[10.1175/1520-0477\(1994\)075<0811:caotum>2.0.co;2](https://doi.org/10.1175/1520-0477(1994)075<0811:caotum>2.0.co;2).
- Li, D.S., Sun, J.H., Fu, S.M., Wei, J., Wang, S.G., Tian, F.Y., 2016. Spatiotemporal characteristics of hourly precipitation over central eastern China during the warm season of 1982–2012. *Int. J. Climatol.* 36, 3148–3160. doi:[10.1002/joc.4543](https://doi.org/10.1002/joc.4543).
- Liao, G.M., Yan, J.P., Hu, N.N., Liu, Y., 2012. Analysis on temporal series of precipitation and drought-flood about the recent 50 years in the east of Sichuan Basin. *Res. Environ. Yangtze Basin* 21, 1161–1166. doi:[10.1007/s11783-011-0280-z](https://doi.org/10.1007/s11783-011-0280-z), (in Chinese).
- Liu, R.X., Sun, J.H., Chen, B.F., 2019. Selection and classification of warm-sector heavy rainfall events over South China. *Chinese J. Atmos. Sci.* 43 (1), 119–130. doi:[10.3878/j.issn.1006-9895.1803.17245](https://doi.org/10.3878/j.issn.1006-9895.1803.17245), (in Chinese).
- Schumacher, R.S., 2011. Ensemble-based analysis of factors leading to the development of a multiday warm-season heavy rain event. *Mon. Wea. Rev.* 139 (9), 3016–3035. doi:[10.1175/MWR-D-10-05022.1](https://doi.org/10.1175/MWR-D-10-05022.1).
- Shao, Y.K., Shen, T.L., You, Y., Kang, L., 2005. Precipitation features of Sichuan Basin in the recent 40 decades. *J. Southwest Agricultural University* 27, 749–752. doi:[10.13718/j.cnki.xdk.2005.06.001](https://doi.org/10.13718/j.cnki.xdk.2005.06.001), (in Chinese).
- Tang, H., Fu, S.M., Sun, J.H., Mai, Z., Jin, S.L., Zhang, Y.C., 2020. Investigation of Severe Precipitation Event Caused by an Eastward-Propagating MCS Originating from the Tibetan Plateau and a Downstream Southwest Vortex. *Chinese Journal of Atmospheric Sciences* 44 (6), 1275–1290. doi:[10.3878/j.issn.1006-9895.1911.19206](https://doi.org/10.3878/j.issn.1006-9895.1911.19206), (in Chinese).
- Tao, S.Y., 1980. *The Torrential Rain in China*. Science Press, Beijing, pp. 1–225 (in Chinese).
- Wang, C.X., Ma, Z.F., Qin, N.S., Zhang, S.Q., Deng, B., 2016. Recognition and spatiotemporal variation of regional rainstorm processes over Sichuan Basin. *Meteorol. Sci. Techn* 44, 777–781. doi:[10.3969/j.issn.1671-6345.2016.05.014](https://doi.org/10.3969/j.issn.1671-6345.2016.05.014), (in Chinese).
- Wang, H.J., Sun, J.H., Wei, J., Zhao, S.X., 2014. Classification of persistent heavy rainfall events over southern China during recent 30 years. *Climatic Environ. Res.* 19, 713–725. doi:[10.3878/j.issn.1006-9585.2013.13143](https://doi.org/10.3878/j.issn.1006-9585.2013.13143), (in Chinese).
- Yu, S.H., 1984. Resultant analysis of large-scale heavy rain storm over Sichuan Basin. *Plateau Meteorol.* 3, 58–67 (in Chinese).
- Zhao, S.X., Tao, Z.Y., Sun, J.H., Bei, N.F., 2004. *Study on mechanism of formation and development of heavy rainfalls on Meiyu front in Yangtze River*. China Meteorological Press, Beijing, pp. 1–281 (in Chinese).
- Zhou, C.Y., Li, Y.Q., Fang, J., Peng, J., 2008. Features of the summer precipitation in the west and east of Sichuan and Chongqing Basin and on the eastern side of the plateau and the relating general circulation. *Plateau Mount. Meteorol. Res.* 28, 1–8. doi:[10.3969/j.issn.1674-2184.2008.02.001](https://doi.org/10.3969/j.issn.1674-2184.2008.02.001), (in Chinese).